High-pressure dynamic, thermodynamic properties, and hardness of CdP_2*

Shi-Quan Feng(冯世全)[1,†], Ling-Li Wang(王伶俐)[1], Xiao-Xu Jiang(姜晓旭)[2], Hai-Nin Li(李海宁)[1], Xin-Lu Cheng(程新路)[2], and Lei Su(苏磊)[1,3,‡]

[1] *The High Pressure Research Center of Science and Technology, Zhengzhou University of Light Industry, Zhengzhou* 450002, *China*
[2] *Institute of Atomic and Molecular Physics, Sichuan University, Chengdu* 610065, *China*
[3] *Key Laboratory of Photochemistry, Institute of Chemistry, Chinese Academy of Sciences, Beijing* 100190, *China*

(Received 25 October 2016; revised manuscript received 28 December 2016; published online 20 February 2017)

Using a pseudopotential plane-waves method, we calculate the phonon dispersion curves, thermodynamic properties, and hardness values of α-CdP_2 and β-CdP_2 under high pressure. From the studies of the phonon property and enthalpy difference curves, we discuss a phase transform from β-CdP_2 to α-CdP_2 in a pressure range between 20 GPa and 25 GPa. Then, the thermodynamic properties, Debye temperatures, and heat capacities are investigated at high pressures. What is more, we employ a semiempirical method to evaluate the pressure effects on the hardness for these two crystals. The results show that the hardness values of both α-CdP_2 and β-CdP_2 increase as pressure is increased. The influence mechanism of the pressure effect on the hardness of CdP_2 is also briefly discussed.

Keywords: high pressure, phase transition, thermodynamic properties, hardness

PACS: 63.20.dk, 05.70.Fh, 67.25.bd **DOI:** 10.1088/1674-1056/26/4/046301

1. Introduction

Cadmium diphosphide, which belongs to the family of II–V group semiconductor compounds, is an important technical material as a wide-gap semiconductor. Due to its superior optical properties, CdP_2 has a wide range of applications in the fabrication of solar cells.[1] In addition, its large thermo-optical coefficient leads to numerous applications in thermal sensors.[2,3] What is more, its wide band gap and anisotropic electrical properties make CdP_2 a promising material in electronic engineering.[4]

Owing to its important practical application values, the properties of CdP_2 have been extensively studied. There are two well-known crystalline phases of cadmium diphosphide, i.e., orthorhombic (α)-CdP_2[5] and tetragonal (β) CdP_2.[6] These two modifications are considered to be stable under ambient conditions. But because β-CdP_2 is more stable than α-CdP_2 at ambient pressure, most of the previous investigations focused on β-CdP_2, especially, on its optical and electrical properties.[7–11] Dynamics of the lattice and thermal properties of β-CdP_2 have also been investigated.[12] In addition, because the defects and doping effect have a strong influence on electrical and optical properties of CdP_2, so a lot of studies[13,14] have been focused on studying the band structure and absorption spectrum of β-CdP_2 with the effects of doping and process-induced defects, and the reported properties of CdP_2 compounds with defects or doping effect differ widely. What is more, the temperature-induced phase transition of CdP_2 crystal has been studied.[15] In our previous work,[16] we investigated the photoinduced non-thermal phase transition of β-cristobalite. In addition, we have predicted the pressure-induced phase transition of CdP_2 crystals.[17]

However, there is little attention being paid to the hardness of CdP_2 under high pressure, especially for α-CdP_2, even the phonon, thermodynamic properties under high pressure have not been reported before. Hence, we will mainly investigate the phonon dispersive curves, thermodynamic properties and hardness values of α-CdP_2 and β-CdP_2 under high pressure in this paper. In addition, we will further study the pressure-induced phase transition of CdP_2 crystal from dynamic properties. What is more, we will discuss the effects of pressure on the hardness for these two formations of CdP_2 crystal.

First-principles calculations within density functional theory (DFT) have been widely used to investigate the structural properties, lattice dynamics and thermodynamic properties for many kinds of crystals.[18,19] In this work, we employ this method to systematically explore the phonon properties, thermodynamic properties and hardness of α-CdP_2 and β-CdP_2. The rest of this paper is organized as follows. In Section 2, the theoretical computational method is briefly described. In Section 3, the results and discussion are presented.

*Project supported by the National Natural Science Foundation of China (Grant No. 11547158) and the Doctoral Fund of Zhengzhou University of Light Industry, China (Grant Nos. 2014BSJJ088 and 2015XJJZ022).

†Corresponding author. E-mail: fengsq2013@126.com
‡Corresponding author. E-mail: 2014079@zzuli.edu.cn

© 2017 Chinese Physical Society and IOP Publishing Ltd

In Section 4, some conclusions are drawn from the present study.

2. Computational methods and details

In this work, the phonon properties, elastic properties, thermodynamic properties, and hardness values of α-CdP_2 and β-CdP_2 are investigated by standard Kohn–Sham self-consistent density functional theory.[20,21] In our study, the experimental lattice parameters for α-CdP_2 and β-CdP_2, cited from Refs. [22] and [23], are used as the initial structure of calculations, respectively. The β-CdP_2 crystallizes in space group $P4_32_12 = D_4$ with lattice parameters $a = b = 5.2852$ Å and $c = 19.787$ Å, and $\beta = 90^\circ$ at a temperature of 293 K; while the α-CdP_2 crystallizes in space group $Pna2_1$ with lattice parameters $a = 9.901$ Å, $b = 5.409$ Å, and $c = 5.157$ Å, and $\beta = 90^\circ$. The structural optimizations for the positions of atoms are carried out by using the conjugate gradient (CG) algorithm, and the self-consistency tolerance is set to be 1×10^{-7} eV for the total energy per atom and 0.03 eV/Å for atomic force in the CG optimization move. For the exchange-correlation energy, we adopt the generalized gradient approximation designed by Perdew, Burke, and Ernzerhof (PBE).[24,25] A pseudopotential plane-wave method is employed to describe the interaction between valence electron and atomic core. In our calculation, the valence electronic configurations for Cd and P are set to be $4d^{10}5s^2$ and $3s^23p^3$, respectively. A plane-wave basis set to be an energy cutoff of 290 eV is closed to ensure a stable state of the system energy. The Brillouin zone sampling is performed by using the Monkhorst–Pack grid.[26]

For phonon calculations, there are two main methods: a frozen-phonon method[27] and a linear-response method.[28,29] In the frozen-phonon method, by exerting a small displacement for each of the atoms of the central cell in different directions, the forces acting on the other atoms can be calculated. Then the phonon dispersion curves can be obtained from supercell calculations by comparing the forces changes before and after the small displacement. In the linear-response approach, the second derivatives of the total energy are obtained by the linear variation of the electron density with application of an external, static, perturbation. Then, according to the first-order perturbation theory, a self-consistent equation between the variation of external potential field and charge density response can be established. By solving the self-consistent equation, the charge density response, dynamical matrix, force constants and phonon frequencies can be calculated. In this paper, we adopt the linear-response method for all the phonon calculations.

In addition, computational methods of thermodynamic properties are shown in Subsection 3.3. What is more, the Vickers hardness values of crystals are calculated by the theoretical method proposed by Gao[30] in 2006, and the calculation method is given in detail in Subsection 3.4.

3. Results and discussion

3.1. Phonon properties and structural transition

As is well known, there are two phases of cadmium diphosphide, i.e., α-CdP_2 and β-CdP_2. These two modifications are considered to be stable under ambient conditions. But little attention has been paid to the hardness of CdP_2 under high pressure. In this work, we investigate the changes of enthalpy value of α-CdP_2 and β-CdP_2 as pressure is increased, and plot the enthalpy difference curves of α-CdP_2 and β-CdP_2 in Fig. 1.

Based on the results of enthalpy difference curves shown in Fig. 1, it is easy to find that β formation is a more stable structure of CdP_2 in a pressure range from 0 GPa to 20 GPa. While as the pressure further increases, the enthalpy value of the α phase becomes smaller than that of the β phase, which means that α-CdP_2 becomes a more stable phase when the pressure is larger than 20 GPa. This may indicate that a phase transition from β to α phase happens at a pressure of just a little over 20 GPa.

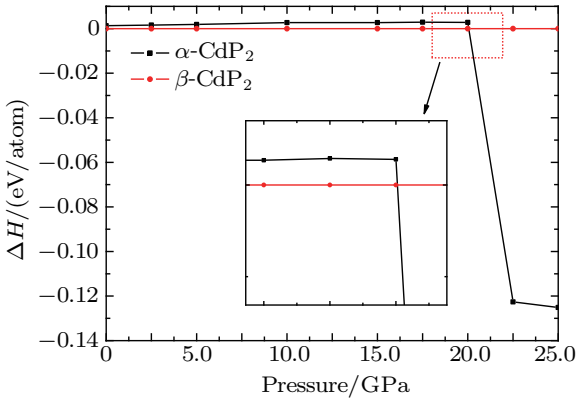


Fig. 1. (color online) Variations of enthalpy difference of α-CdP_2 and β-CdP_2 with pressure at 298 K. With the enthalpy value of β-CdP_2 used as a reference, we set the enthalpy value of β-CdP_2 at different pressures to be zero marked by a red line, then the black line corresponds to the enthalpy difference between α-CdP_2 and β-CdP_2.

A phonon dispersion curve is an important approach to studying the lattice dynamics. To confirm our guess, we calculate the phonon dispersion curves of β-CdP_2 and α-CdP_2 at several different pressures. Figures 2 and 3 show our calculated results. From Fig. 1, it can be seen that the lattice dynamics of β-CdP_2 exhibits a variety of anomalies. (i) It is interesting to note that the phonon frequencies of optical branches increase as pressure increases, while the acoustic phonon branches soften as pressure increases. (ii) When the pressure is raised to 20 GPa, an imaginary frequency appears at the M point. As the pressures further increases, the whole transverse acoustic (TA) branches soften to imaginary frequencies at 25 GPa, which indicates a structural instability of β-CdP_2 under high pressure.

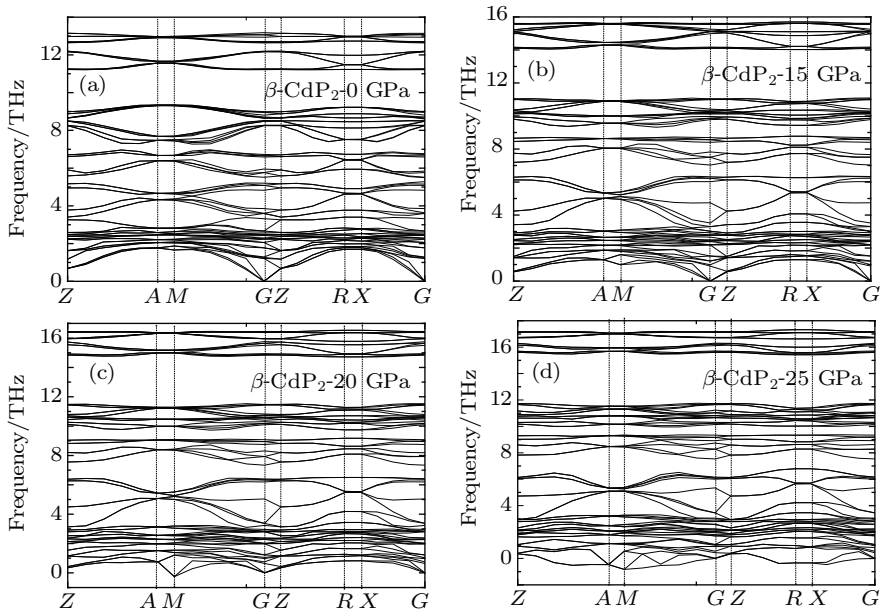


Fig. 2. Phonon dispersion curves of β-CdP_2 at different pressures.

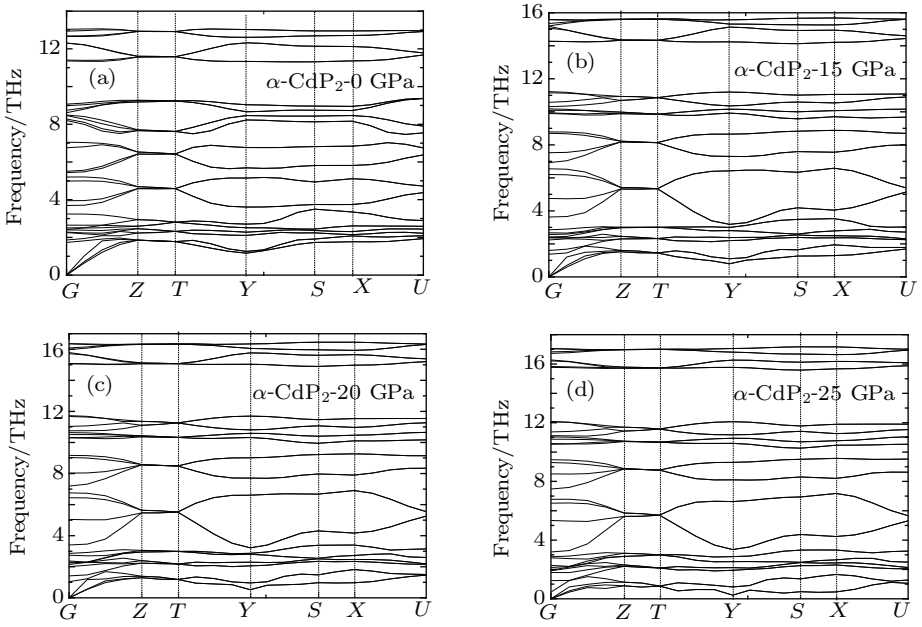


Fig. 3. Phonon dispersion curves of α-CdP_2 at different pressures.

For α-CdP_2, the phonon calculations predicted that it is stable from 0 GPa to 25 GPa. While for β-CdP_2, the appearance of the imaginary frequency in the phonon spectrum at a pressure larger than 20 GPa indicates that it becomes unstable under high pressure.

Combining the phonon dispersion curves with the enthalpy difference curves of α-CdP_2 and β-CdP_2, it can be determined that a phase transition from β phase to α phase occurs at a pressure slightly larger than 20 GPa. Before phase transition, the α-CdP_2 is a metastable phase. At a pressure larger than 20 GPa, α-CdP_2 becomes a more stable phase than β-CdP_2. The transition pressure corresponds to the intersection point of enthalpy difference curve shown in Fig. 1.

3.2. Mechanical stability

In order to show the rationality of our research for CdP_2 transition, we calculate the elastic properties of these two phases in a pressure range between 0 GPa and 25 GPa to investigate their mechanical stabilities.

For α-phase, the mechanical stability criteria[31] are as follows:

$$\begin{aligned} &C_{11}>0,\ C_{22}>0,\ C_{33}>0,\ C_{44}>0,\ C_{55}>0,\ C_{66}>0,\\ &C_{11}+C_{22}-2C_{12}>0,\quad C_{11}+C_{33}-2C_{13}>0,\\ &C_{22}+C_{33}-2C_{23}>0. \end{aligned} \tag{1}$$

For the β-phase, the mechanical stability criteria are given as

follows:

$$C_{11}-C_{12}>0,\ \ (C_{11}+C_{12})C_{33}-2C_{13}^2>0,\ \ C_{66}>0. \quad (2)$$

The elastic constants of α-CdP_2 and β-CdP_2 at zero pressure are presented in Table 1.

Table 1. Elastic constants of α-CdP_2 and β-CdP_2 at zero pressure.

	C_{11}	C_{22}	C_{33}	C_{44}	C_{55}	C_{66}	C_{12}	C_{13}	C_{23}
α-CdP_2	101.3	91.4	87.3	37.4	28.2	19.0	31.1	37.7	32.5
β-CdP_2	92.6	92.6	102.2	36.2	36.2	41.1	33.2	32.3	32.3

Combining the results listed in Table 1 with the mechanical stability criteria presented in Eqs. (1) and (2), it is not difficult to judge that both α-CdP_2 and β-CdP_2 are stable in mechanics. Further studies show that these two phases are mechanically stable in our research pressure range.

3.3. Thermodynamic properties

The Debye temperature of a solid is an important physical quantity of thermodynamic properties, it is closely related to the hardness and superconducting transition temperature of material. So the research of Debye temperature has an important physical significance. The Debye temperature can be obtained from elastic constants by following equation:

$$\Theta=\frac{\mathrm{h}}{\mathrm{k_B}}\left[\frac{3n}{4\pi}\left(\frac{N_\mathrm{A}\rho}{M}\right)\right]^{1/3}V_\mathrm{m}, \quad (3)$$

where h is the Planck constant, k_B is the Boltzmann constant, N_A is theAvogadro constant, n is the number of atoms in the cell, M is the molar mass, ρ is the density, and V_m is the average wave velocity, which can be calculated from the following formula:

$$V_\mathrm{m}=\left[\frac{1}{3}\left(\frac{2}{V_\mathrm{s}^3}+\frac{1}{V_\mathrm{p}^3}\right)\right]^{-1/3}, \quad (4)$$

where V_s and V_p are the shear wave velocity and compressional wave velocity, respectively.

According to the above formula and the results of elastic constants, we further obtain the Debye temperatures of two formations of CdP_2 crystal at high pressures. Figure 4 shows the calculated Debye temperatures of CdP_2 varying with temperature at different pressures. It is noted that the Debye temperatured of α-CdP_2 and β-CdP_2 increase as pressure increases.

The heat capacity of a solid, as an old topic of the condensed matter physics, follows the standard elastic continuum theory:[32] the heat capacity C_v is proportional to T^3 at sufficiently low temperatures; while at a higher temperature, the heat capacity C_v approaches to the Petit–Dulong limit.[33] Figure 5 shows plots of heat capacity $C_v(T)$, versus temperature, for α-CdP_2 and β-CdP_2 at different pressures. It can be seen from Fig. 5 that the heat capacity C_v decreases as pressure increases at low temperatures. However, at higher temperatures, C_v is still close to the Petit-Dulong limit at different pressures.

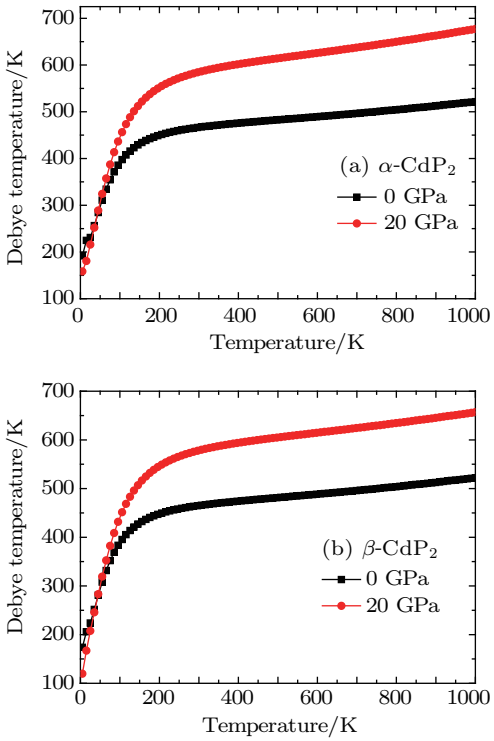


Fig. 4. (color online) Variations of Debye temperature with temperature of two formations of CdP_2 crystal under high pressures.

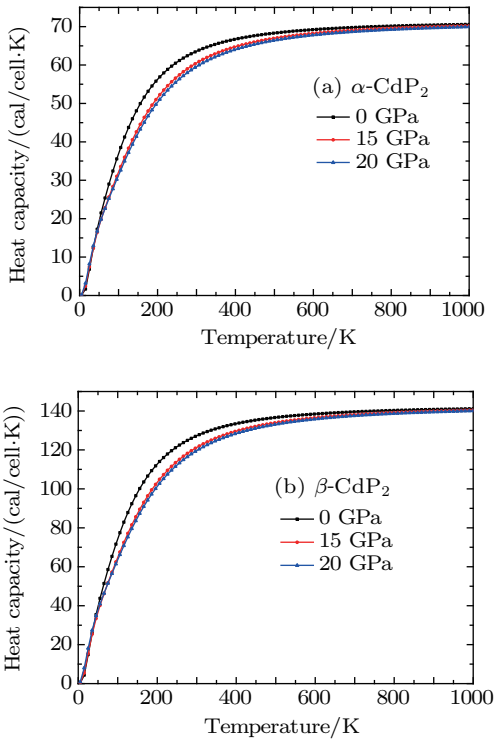


Fig. 5. (color online) Variations of heat capacity with temperature for α-CdP_2 and β-CdP_2 at different pressures.

3.4. Hardness

Vickers hardness, as a physical property to measure the shearing resistance and compression resistance of a solid ma-

terial, is commonly defined as the ratio of F/A; where F is the pressed force applied to the diamond indenter in the unit of kilograms-force, and A is the indentation area on the surface of a measured material in the unit of square millimeter. In this work, we calculate the Vickers hardness values of α-CdP_2 and β-CdP_2 from 0 GPa to 20 GPa by the microscopic theoretical model proposed by Gao.[30] In this model, the Vickers hardness can be calculatedfrom the following formulas:

$$H_{\rm v} = \left[\prod^{\mu}(H_{\rm v}^{\mu})^{N^{\mu}}\right]^{1/\Sigma N^{\mu}}, \tag{5}$$

$$H_{\rm v}^{\mu} = 699P^{\mu}(v_{\rm b}^{\mu})^{-5/3}\exp(-3005f_{\rm m}^{1.553}), \tag{6}$$

where $H_{\rm v}$ is the hardness of the calculated material, $H_{\rm v}^{\mu}$ is the hardness of μ-type bond in the calculated material, N^{μ} is the total bond number in the cell, P^{μ} is the Mulliken overlap population of μ-type bond, $v_{\rm b}^{\mu}$ is the bond volume, and $f_{\rm m}$ is the metallicity. The value of $v_{\rm b}^{\mu}$ can be calculated from the following formula:

$$v_{\rm b}^{\mu} = \frac{(d^{\mu})^3}{\sum_{v}(d^{v})^3(N^{v}/\Omega)} = \frac{(d^{\mu})^3\Omega}{\sum_{v}[(d^{v})^3N^{v}]}, \tag{7}$$

where d^{μ} is the bond length and Ω is the cell volume.

The metallicity $f_{\rm m}$ is approximate to $n_{\rm m}/n_{\rm e}$, where $n_{\rm m}$ and $n_{\rm e}$ are the number of electrons that can be excited and the total number of the valence electrons, respectively. According to the electronic Fermi liquid theory, $f_{\rm m}$ can be expressed as follows:

$$f_{\rm m} = \frac{n_{\rm m}}{n_{\rm e}} = \frac{0.026D_{\rm F}}{n_{\rm e}}, \tag{8}$$

where $D_{\rm F}$ is the electron density of states at the Fermi level.

According to the above theory, we calculate the bond parameters and Vickers hardness values of α-CdP_2 and β-CdP_2 at ambient pressure. The P–P and Cd–B bond parameters as well as the Vickers hardness values are listed in Table 2. From Table 2, it is not difficult to find that the contribution of the P–P bonds plays a major role in determining the hardness values of α-CdP_2 and β-CdP_2, while the Cd–P bonds limit their hardness values. In addition, the metallicity $f_{\rm m}$ is an important factor to limit their hardness values. With the increase of the metallicity of material, the hardness decreases.

Table 2. Calculated bond parameters and Vickers hardness values of α-CdP_2 and β-CdP_2 at ambient pressure.

	Bond	d^{μ}/Å	P^{μ}	Ω/Å^3	$v_{\rm b}^{\mu}$/Å^3	$f_{\rm m}/10^{-3}$	$H_{\rm v}^{\mu}$/GPa	$H_{\rm v}$/GPa
α-CdP_2	P–P	2.162	0.62	286.0	7.802	0	14.12	3.84
	P–P	2.208	0.49		8.310	0	10.05	
	Cd–P	2.584	0.53		13.320	1.713	4.16	
	Cd–P	2.616	0.44		13.821	1.713	3.25	
	Cd–P	2.626	0.10		13.980	1.713	0.72	
	Cd–P	2.644	0.33		14.269	1.713	2.31	
β-CdP_2	P–P	2.168	0.60	574.1	7.873	0	13.461	4.59
	P–P	2.214	0.50		8.385	0	10.099	
	Cd–P	2.583	0.58		13.315	1.078	4.979	
	Cd–P	2.621	0.43		13.911	1.078	3.431	
	Cd–P	2.633	0.16		14.103	1.078	1.248	
	Cd–P	2.638	0.42		14.183	1.078	3.245	

In order to study the effect of pressure on the hardness property of CdP_2, we calculate the Vickers hardness values in a pressure range from 0 GPa to 20 GPa. The results are shown in Table 3. It is noted that the hardness values of α-CdP_2 and β-CdP_2 increase as pressure is increased. By analyzing the bond parameters and electronic properties of α-CdP_2 and β-CdP_2, we find that the hardness is most closely related to the chemical bonds and structural symmetry of crystal. While the pressure has almost no effect on the structural symmetry of crystal, it mainly affects their chemical bonds. Further analysis shows that there are three reasons for explaining the increasing hardness at high pressure: 1) the hardness of covalent bond (P–P bond) increases as pressure is increased; 2) the hardness of ionic bond (Cd–P bond) increases as pressure is increased; 3) the metallicity of CdP_2 is weakened as pressure is increased. In a word, due to the enhancement of covalent bonds and the weakening of metal bonds, the hardness values of α-CdP_2 and β-CdP_2 are increased at a higher pressure.

Table 3. Calculated Vickers hardness value of α-CdP_2 and β-CdP_2 at different pressures.

Compounds	0 GPa	5 GPa	10 GPa	15 GPa	20 GPa
α-CdP_2	3.84	4.76	5.71	6.28	6.71
β-CdP_2	4.59	5.42	5.98	6.40	6.74

4. Conclusions

In this work, by calculating the phonon properties and enthalpy difference between α-CdP_2 and β-CdP_2 at high pressures, a pressure-induced phase transition of $CdP_2$is confirmed in a pressure range between 20 GPa and 25 GPa in theory. In addition, the studies of elastic properties show that α-CdP_2 and β-CdP_2 are stable in mechanics in our studied pressure

range. The investigations of thermodynamic properties show that the heat capacity decreases and the Debye temperature increases as pressure increases.

What is more, we discuss the pressure effects on the hardness of α-CdP_2 and β-CdP_2. The results show that both the hardness values of covalent bonds (P–P bonds) and ionic bonds (Cd–P bonds) increase as pressure is increased, while the metallicity is weakened as pressure is increased. This causes the hardness values of both α-CdP_2 and β-CdP_2 to increase as pressure is increased. As the pressure rises from 0 GPa to 20 GPa, the Vickers hardness of α-CdP_2 increases from 3.84 GPa to 6.71 GPa. While the Vickers hardness of β-CdP_2 increases from 4.59 GPa to 6.74 GPa. From this conclusion, it is easy to find that the effect of pressure plays an important role in the hardness of CdP_2 crystal; it can change the hardness of the material by affecting its chemical bonds.

References

[1] Dmitruk N L, Zuev V A and Stepanova M A 1991 *Russ. Phys. J.* **34** 642

[2] Aleinikova K B, Kozlov A I, Kozlova S G and Sobolev V V 2002 *Fiz. Tverd. Tela.* **44** 1206

[3] Trukhan V M, Sheleg A U and Fekeshgazi I F 2004 *Photoelectronics* **13** 15

[4] Lazarev V B, Shevchenko V Y, Grinberg L K and Sobolev V V 1976 *Group II–V Semiconductor Compounds* (Moscow: Nauka)

[5] Olofsson O and Gullman J 1970 *Acta Cryst. B* **26** 1883

[6] Horn H 1969 *Bull. Acad. Polon. Sci., Ser. Sci. Chim.* **17** 69

[7] Kudin A P 2002 *Inorg. Mater.* **38** 640

[8] Baran J, Pasechnik Yu A, Shportko K V, Trzebiatowska-Gusowska M and Venger E F 2006 *J. Mol. Struct.* **792** 239

[9] Januskevicius Z, Korec N, Sakalas A and Tychina I 1981 *Phys. Status Solidi A* **65** 149

[10] Vengera E F, Pasechnikb Yu A and Shportkob K V 2005 *J. Mol. Struct.* **744** 947

[11] Gnatyuk1 V A, Borshch V V, Kuzmenko M G, Gorodnychenko O S and Yuryev S O 2004 *Phys. Chem. Solids State* **5** 256

[12] Kopytov A V, Polygalov Y I and Tkachenko V N 2005 *Russ. Phys. J.* **48** 679

[13] Trukhan V M, Soshnikov L E, Marenkin S F and Haliakevich T V 2005 *Inorg. Mater.* **41** 901

[14] Korets M S 1999 *Ukr. Fiz. Zh.* (Ukr. Edn.) **44** 738

[15] Marenkin S F, Soshnikov L E and Trukhan V M 2005 *Russ. J. Inorg. Chem.* **50** s41

[16] Feng S Q, Zang H P, Wang Y Q, Cheng X L and Yue J S 2016 *Chin. Phys. B.* **25** 016701.

[17] Feng S Q and Cheng X L 2011 *Comput. Theor. Chem.* **966** 149

[18] Fan T, Zeng Q F and Yu S Y 2016 *Acta Phys. Sin.* **65** 118102 (in Chinese)

[19] Wang X X, Zhao L T, Cheng H X and Qian P 2016 *Acta Phys. Sin.* **65** 057103 (in Chinese)

[20] Ordejón P, Artacho E and Soler J M 1996 *Phys. Rev. B* **53** R10441

[21] Strobel R, Maciejewski M, Pratsinis S E and Baiker A 2006 *Therm. Acta* **445** 23

[22] Lazarev V B, Shevchenko V Y, Greenberg J H and Sobolev V V 1978 *Poluprovodnikovye soedineniya gruppy AIIBV (II–V Semiconductors)* (Moscow: Nauka)

[23] Olofsson O and Gullman J 1970 *Acta Cryst. B* **26** 1883

[24] Wu Z G and Cohen R E 2006 *Phys. Rev. B* **73** 2351161

[25] Perdew J P, Burke K and Ernzerhof M 1996 *Phys. Rev. Lett.* **77** 3865

[26] Monkhorst H J and Pack J D 1976 *Phys. Rev. B* **13** 5188

[27] Kunc K and Martin R M 1982 *Phys. Rev. Lett.* **48** 406

[28] Giannozzi P, Gironcoli S, Pavone P and Baroni S 1991 *Phys. Rev. B* **43** 7231

[29] Gonze X and Lee C 1997 *Phys. Rev. B* **55** 10355

[30] Gao F M 2006 *Phys. Rev. B* **73** 132104

[31] Speziale S, Jiang F, Caylor C L, Kriminski S, Zha C S, Thorne R E and Duffy T S 2003 *Biophys. J.* **85** 3202

[32] Debye P 1912 *Ann. Phys.* **39** 789

[33] Petit A T and Dulong P L 1819 *Ann. Chim. Phys.* **10** 395